A microcontroller-based lock-in amplifier for sub-milliohm resistance measurements

Lars E. Bengtsson
Department of Physics, University of Gothenburg, SE-412 96 Gothenburg, Sweden

(Received 27 March 2012; accepted 13 June 2012; published online 6 July 2012)

This paper presents a novel approach to the design of a digital ohmmeter with a resolution of $<60\ \mu\Omega$ based on a general-purpose microcontroller and a high-impedance instrumentation amplifier only. The design uses two digital I/O-pins to alternate the current through the sample resistor and combined with a proper firmware routine, the design is a lock-in detector that discriminates any signal that is out of phase/frequency with the reference signal. This makes it possible to selectively detect the μV drop across sample resistors down to 55.6 $\mu\Omega$ using only the current that can be supplied by the digital output pins of a microcontroller. This is achieved without the need for an external reference signal generator and does not rely on the computing processing power of a digital signal processor. © *2012 American Institute of Physics*. [http://dx.doi.org/10.1063/1.4731683]

I. INTRODUCTION

Lock-in amplifiers (LIAs) have been used in physics laboratories for a long time and with their extreme signal selectivity, with Q-values of the order of 10^6, they are used in such a wide variety of applications as low level optical experiments, acoustical and cross-talk measurements, electron spectroscopy, radio astronomy, neurologic research, feedback control of lasers, complex impedance measurements, optical pyrometry, hot wire anemometry, and photon counting.[1,2] They are also used for measurements of very low real and complex impedances, for example, in superconducting squid measurements[1] and measurements of the frequency dependence of impedance in ac coupled cricuits.[3] Feng *et al.*[4] designed an analog lock-in amplifier for low-resistance measurements at cryogenic temperatures. This paper will demonstrate how this design can be simplified considerably by designing a digital, microcontroller-based LIA for the measurement of very low resistances.

Resistance is typically measured by taking advantage of Ohm's law; a known current is injected into the resistor and the voltage drop across the resistor is measured with a voltmeter. In order to measure resistances in the milliohm or sub-milliohm ranges, special care must be taken to avoid measurement errors. First of all, the wiring resistance must be eliminated by using the 4-wire technique[5] (a *Kelvin probe*).

Another problem that has to be addressed in micro- or milliohm measurements is the fact that the voltage drop across the resistor will be very small. A 100 mA current will cause a 100 μV drop across a 1 mΩ resistor. If possible, the current could be increased, but some samples may not allow the increase in heat loss due to the increased current[4] and many applications are simply forced to deal with very low signal levels.[6] Signals in the sub-mV range are also of the same size as typical noise sources such as Johnson noise and 1/f-noise.[7] The signal can be amplified, however a general, non-selective amplifier will amplify the noise as well as the signal. The voltage over the resistance can be measured using a phase lock-in technique that will separate the signal from noise.[8–10] In traditional lock-in theory, the experiment is excited by a reference signal, $r(t)$, and by multiplying the reference signal with the measurement signal, $m(t)$, a series of sum and difference signal frequencies are produced where the difference signal component corresponding to the measurement signal will have frequency 0, i.e., it is a dc signal and is easily separated from the other signals with a narrow-band low-pass filter, see Figure 1.

However, analog electronic multipliers are complex, expensive, and may suffer from nonlinearities.[1] For that reason, other solutions have been suggested,[8,9,11] see Figure 2.

When the square wave is "on" the switch is in the upper position and when it is "off" it is in the lower position (and the signal is phase-shifted 180°). If $m(t)$ and $r(t)$ are "in-phase," this switching will rectify $m(t)$ and the RC-filter will smooth it. Notice that signals with a frequency not exactly equal to the frequency of $r(t)$ will be averaged to zero by the low-pass filter. The design in Figure 2 is indeed a phase sensitive device that will discriminate any signals that do not have the right frequency and phase. This was the principle of Feng *et al.'s*[4] design.

Digital LIAs can be divided into two classes; those which use a digital signal processor (dsp) (with real-number multiplication in hardware, floating or fixed point) and those which use general purpose integer processors. If the digital LIAs has access to the processing power of a dsp, the multiplication of $r(t)$ and $m(t)$ can be implemented directly in firmware. This has been demonstrated, for example, by Restelli *et al.*,[2] by designing a digital LIA based on a Xlinx field programmable gate array for photon counting, and by Tashev,[12] who used a Motorola 5600 dsp to design a digital LIA with numerical multiplication. Judging from published works in the field, Texas Instruments TMS320 series of dsps seem to be the most commonly used digital multiplier in digital LIAs.[13,14]

Firmware implementations of the lock-in technique have also been suggested.[15–19] A phase sensitive detector (PSD) implemented in firmware samples the signal $m(t)$ twice during the reference signal's period. These samples are separated by

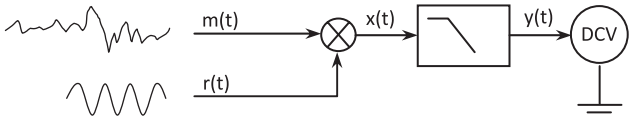

FIG. 1. Lock-in: Multiply and filter.

a time corresponding to π radians. If the frequency of the reference signal agrees with the frequency of the measurement signal, then the two samples will have different signs and if subtracted the signal will be enhanced[14] while signals with frequencies that differ from that of the reference signal will be discriminated over time if many samples are averaged, see Figure 3.

Li *et al.*[18] recently demonstrated that by sampling twice as fast (samples separated by $\pi/2$), both the "in-phase" and the "quadrature" signals could be recovered in order to find both the signal amplitude and the phase shift between $m(t)$ and $r(t)$.

This paper will demonstrate how a digital low-ohmmeter with micro-ohm resolution can be designed by implementing a combination of the hardware and firmware phase-locking techniques described above in a microcontroller design.

The rest of this paper is organized as follows: Sec. II describes the hardware and firmware principles that are used. Section III analyzes the system from a theoretical point of view and Sec. IV describes the methods and materials used in the design and implementation of the digital ohmmeter. Experimental results are presented in Sec. V, Sec. VI contains a discussion of the design and experimental results, and Sec. VII summarizes the paper with the most important conclusions.

II. MICROCONTROLLER LOCK-IN

A. Hardware

This paper suggests the digital design for lock-in detection in Figure 4.

I/O-pins 1 and 2 will be configured as digital outputs and alternately set high and low; this will produce an alternating bipolar signal through the chain of resistors R_0-R_X-R_1. During phase 1, I/O-port 1 is set high and I/O-pin 2 is set low and during phase two, both outputs are inverted. The rate at which this switching occurs corresponds to the lock-in frequency. R_X is the unknown resistor (of the order of mΩ) and the R_0,R_1-resistors (150 Ω nominal) are necessary to limit the current; digital I/O-pins on typical microcontrollers can only generate currents of the order of 10–20 mA.[20] The instrument amplifier amplifies the voltage drop across R_X. The resistor network consisting of the R_2-R_4 resistors forms a bipolar-to-unipolar converter.[21] This is necessary because the instrument

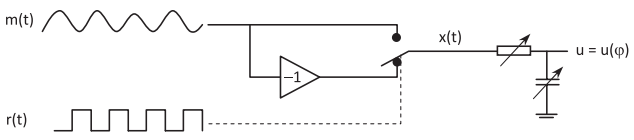

FIG. 2. Phase sensitive detector.

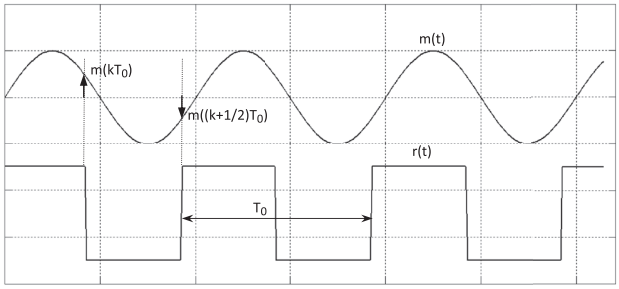

FIG. 3. Firmware PSD: Take samples separated by $0.5T_0$ and subtract pair-wise.[15]

amplifier output signal is bipolar, but the embedded analog-to-digital (ADC) of any microcontroller is unipolar.

B. Firmware

The software is straightforward; first I/O-pin 1 is set to logic high and I/O-pin 2 is set to logic low. This will generate a positive signal output on the instrument amplifier and the ADC input is sampled once (sample s_1). Before the AD conversion is initiated, it is important to allow enough time for the amplifier output to settle. Next, the current through the resistor network is reversed by setting I/O-pin 1 to logic low and I/O-pin 2 to logic high. This will generate a negative signal output on the instrument amplifier and the ADC takes sample number 2 (s_2). These two samples are then subtracted, $s = s_1 - s_2$, and the sample s corresponds to the rectified signal $x(t)$ in Figure 2. By averaging a large number of such samples the low-pass filter in Figure 1 is also synthesized and this completes the lock-in design. Figure 5 illustrates the firmware flowchart.

Notice in Figure 5 how each sample is subtracted by 512. The reason for that is that the embedded 10-bit ADC is unipolar and produces positive integers only. However, the signal conditioning electronics converts negative voltages in the range [−10,0] V into positive voltages in the range [0,2.5] V. Since the reference voltage of the ADC is +5 V, 2.5 V corresponds to the integer 512 in a 10-bit ADC. So, to recover a negative voltage at the instrument amplifier's output, 512 must be subtracted from the ADC integer. In the application described later, 500 samples were averaged, hence the divide-by-500.

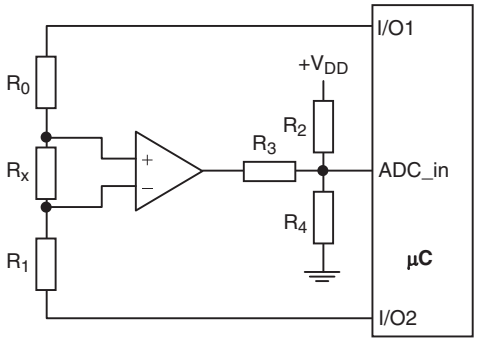

FIG. 4. Digital lock-in amplifier for sub-milliohm measurements.

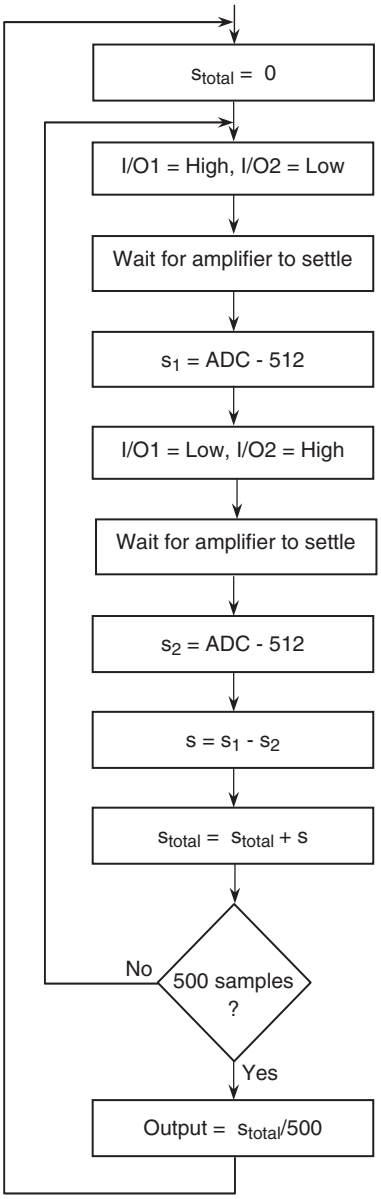

FIG. 5. Digital lock-in amplifier: Firmware flowchart.

III. SYSTEM ANALYSIS

A. Hardware

The resistor network R_2-R_4 in Figure 4 is a bipolar-to-unipolar converter[21] that allows us to analyze negative signals with a unipolar ADC, see Figure 6.

The circuit in Figure 6 produces a unipolar signal according to

$$U_{out} = U_0 + k \times U_{in} = 2.5 + \frac{1}{4}U_{in}. \quad (1)$$

Since the unknown resistor R_X is of the order of mΩ, the voltage drop across it is very small and it is important to keep the current through it as large as possible (assuming the sample tolerates the increase in temperature due to the increased power loss). The limiting factor here is the maximum current sourcing capability of the microcontroller's I/O-pins. The R_0 and R_1 resistors should be chosen large enough to protect the sample from overheating and small enough to generate a large enough voltage drop across the R_X resistor. This design used $R_0 = R_1 = 150\ \Omega$, but they have to be determined for every individual case, depending on how sensitive the sample is to heating due to power loss.

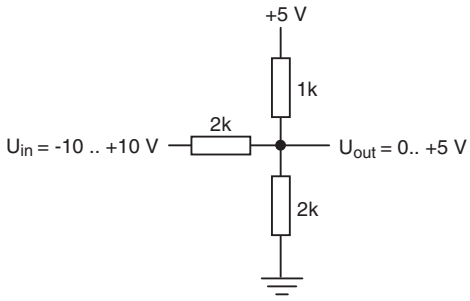

FIG. 6. Bipolar-to-unipolar converter.[21]

If R_0 and R_1 are of the order of $10^2\ \Omega$ and R_X is of the order of $10^{-3}\ \Omega$, the current through the sample is constant (down to the 5th digit). The following notations are now introduced: V_{OH} = the output voltage of an I/O-pin when set high, V_{OL} = the output voltage of an I/O-pin when set low, R_{OH} = the output impedance of an I/O-pin set high, and R_{OL} = the output impedance of an I/O-pin set low. This gives us the equivalent circuit in Figure 7 when I/O-pin 1 is set high.

Hence, if one of the I/O-pins is set high and the other one is set low, the current through the R_0-R_X-R_1 network is

$$i = \frac{V_{OH} - V_{OL}}{R_{OH} + R_0 + R_1 + R_{OL}} = \frac{V_{OH} - V_{OL}}{R_{OH} + 2R_0 + R_{OL}}. \quad (2)$$

(Since $R_0 = R_1$ and, $R_0 R_1 \gg R_X$.) This will cause a voltage drop across R_X

$$U_X = i R_X = \frac{R_X}{R_{OH} + 2R_0 + R_{OL}} \times (V_{OH} - V_{OL}). \quad (3)$$

If the normal mode amplification of the instrument amplifier is A^+_{NM}, the voltage on the instrumentation amplifier's output is

$$U_{in+} = A^+_{NM} \times U_X = \frac{A^+_{NM}(V_{OH} - V_{OL})}{R_{OH} + 2R_0 + R_{OL}} \times R_X. \quad (4)$$

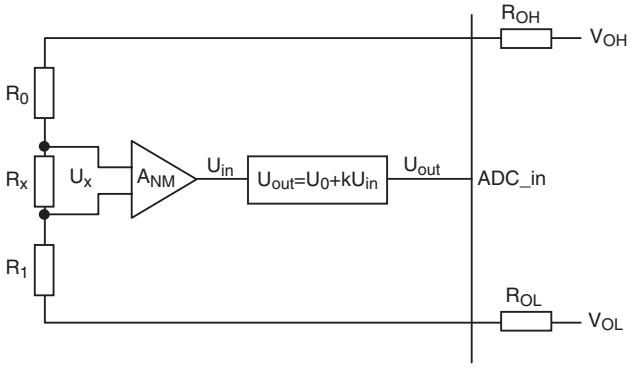

FIG. 7. Equivalent circuit.

To get the voltage sampled by the ADC, (4) is inserted into (1)

$$U_{out+} = U_0 + k \times U_{in+} = U_0 + k \times \frac{A^+_{NM}(V_{OH} - V_{OL})}{(R_{OH} + 2R_0 + R_{OL})} \times R_X, \quad (5)$$

where U_{out+} indicates the current direction. If the current in the R_0-R_X-R_1 network is reversed, the "+" sign in (5) turns into a "−" sign and this voltage is denoted U_{out-}

$$U_{out-} = U_0 - k \times U_{in} = U_0 - k \times \frac{A^-_{NM}(V_{OH} - V_{OL})}{(R_{OH} + 2R_0 + R_{OL})} \times R_X. \quad (6)$$

Expressions (5) and (6) assume that the microcontroller parameters V_{OH}, V_{OL}, R_{OH}, and R_{OL} are identical for all I/O-pins, but allows for a discrepancy in the normal mode amplification of inputs of the same magnitude but different signs.

If the voltages in (5) and (6) are sampled by an n-bit ADC with reference voltage U_{ref}, it will produce integers N_+ and N_-, respectively,

$$N_+ = \frac{U_{out+}}{U_{ref}} \times 2^n, \quad (7)$$

$$N_- = \frac{U_{out-}}{U_{ref}} \times 2^n. \quad (8)$$

(The right-hand sides are rounded to nearest integer by the ADC.) In order to recover the bipolar voltage at the instrument amplifier's output, 2^{n-1} is subtracted from the integers in (7) and (8) in the firmware algorithm, see Figure 5. Hence, each sample s in the firmware flowchart in Figure 5 is an integer determined by the following expression:

$$s = N_+ - 2^{n-1} - (N_- - 2^{n-1}) = N_+ - N_- = \frac{(U_{out+} - U_{out-})}{U_{ref}} \times 2^n = \frac{k \times (V_{OH} - V_{OL}) \times \left(A^+_{NM} + A^-_{NM}\right) \times R_X}{(R_{OH} + 2R_0 + R_{OL}) \times U_{ref}} \times 2^n. \quad (9)$$

Expression (9) indicates that the subtraction of 2^{n-1} in firmware cancels and could be omitted (but was included since the firmware used a general purpose bipolar ADC-routine developed in a previous project). The unknown resistance is solved from (9)

$$R_X = \frac{(R_{OH} + 2R_0 + R_{OL}) \times U_{ref}}{k \times (V_{OH} - V_{OL}) \times \left(A^+_{NM} + A^-_{NM}\right)} \times \frac{s}{2^n}. \quad (10)$$

B. Error analysis

The uncertainty of the absolute resistance measurement needs to be estimated. Consider expression (10)

$$R_X = f\left(R_{OH}, R_0, R_{OL}, U_{ref}, k, V_{OH}, V_{OL}, A^+_{NM}, A^-_{NM}\right). \quad (11)$$

If each one of these parameters have a standard uncertainty of u_i, then the standard uncertainty of R_X is[33,34]

$$u_{Rx} = \sqrt{\sum_i (c_i u_i)^2}, \quad (12)$$

where c_i is the sensitivity coefficient[33,34]

$$c_i = \left|\frac{\partial f}{\partial x_i}\right|. \quad (13)$$

(x_i represents anyone of the parameters in (11).) Parameters R_{OH}, R_{OL}, R_0, V_{OH}, V_{OL}, k, and U_{ref}, were all measured with a digital multimeter (Phillips PM2534) and the standard uncertainties of these measurements were estimated from the multimeter data sheet. (R_{OH}, R_{OL} were measured as described by Reverter *et al.*[35]) s is the sample integer produced by the firmware and has a quantization uncertainty of ±1 counts (uniform distribution) which corresponds to a standard uncertainty of[33,34] $1/\sqrt{3}$.

The gain of the instrumentation amplifier is $1 + 50\ \text{k}/R_G$, where R_G is an external gain resistor chosen by the user.[22] R_G (= two parallel 10 Ω-resistors) were measured with an Agilent 34401A DMM (4-wire method) to 4.986 ± 0.002 Ω (1-σ) which gives a nominal amplification of 10 029 ± 4 (where the ±4 is from the uncertainty in the gain resistor). The data sheet[22] does not specify the uncertainty of a nominal amplification of 10 029 but it does specify that the uncertainty is ±2% for a gain of 1000. If that number is also used for the 10 029 times amplification (= ±201), it would correspond to a standard uncertainty of $201/\sqrt{3} = 116$, and hence the uncertainty due to the gain resistor's uncertainty is negligible.

The factor k was determined by experimental data and using curve fitting (in MATLAB). Notice that the uncertainty depends on s and needs to be calculated for each sample s. In order to get an idea of the size of the uncertainty, the calculations below are for the case $s = 512$ (mid-range). Expressions (12) and (13) indicate that the values of no less than nine partial derivatives need to be calculated for the uncertainty budget. The calculations are extensive but straightforward. Table I summarizes the uncertainty budget for expression (10) when $s = 512$.

Hence, for the midrange value $s = 512$, the theoretically predicted resistance is 38.13 ± 0.32 mΩ, where the uncertainty interval corresponds to one standard uncertainty. If the values in Table I are inserted into expression (10), an

TABLE I. Uncertainty budget.[33,34]

Parameter	Value	Stand. Uncert. (u)	Sens. Const. (c)	u × c
U_{ref}	5.1254 V	0.30 mV	7.46×10^{-3}	2.24×10^{-6}
V_{OH}	5.0579 V	0.30 mV	7.56×10^{-3}	2.27×10^{-6}
V_{OL}	3.91 mV	2.31 μV	7.56×10^{-3}	1.75×10^{-8}
R_0	150.0526 Ω	0.07 Ω	2.04×10^{-4}	1.43×10^{-5}
R_{OH}	57.023 Ω	0.032 Ω	1.02×10^{-4}	3.26×10^{-6}
R_{OL}	17.999 Ω	0.43 Ω	1.02×10^{-4}	4.39×10^{-5}
k	0.24871	0.00014	0.154	2.16×10^{-5}
A_{NM}^{+}	10 029	116	1.90×10^{-6}	2.21×10^{-4}
A_{NM}^{-}	10 029	116	1.90×10^{-6}	2.21×10^{-4}
s	512	0.577	7.47×10^{-5}	4.32×10^{-5}
R_X	38.1295 mΩ	...	...	0.32 mΩ

expression for R_X is achieved

$$R_X = 74.5 \times s\mu\Omega, \tag{14}$$

which suggests a potential resolution of 74.5 $\mu\Omega$/count. These numbers will be commented on later.

IV. METHODS AND MATERIALS

The microcontroller used was a PIC18F4580 (Ref. 20) from Microchip. This is an 8-bit, general purpose controller in a 40-pin DIL package. Figure 8 illustrates the complete circuit diagram.

The microcontroller was clocked with a 15 MHz crystal and the instrumentation amplifier was an INA128 (Ref. 22) from Burr-Brown with a differential input impedance of 10 GΩ. It was configured for maximum normal mode amplification (10 000) with the two 10 Ω-resistors across pins 1 and 8 in Figure 8. A transistor-transistor logic-to-universal serial bus (USB) chip from FTDI (Ref. 23) was used to send data to a host personal computer (PC) via the asynchronous serial port of the microcontroller. This Future Technology Devices International (FTDI) chip converts the PC's USB port into a virtual COM port.

In Figure 8, R_X has been implemented as a potentiometer. This "potentiometer" was a 900 mm long copper wire with a nominal diameter of 0.6 mm and it was used to calibrate the system; the negative input of the instrumentation amplifier was connected to the potentiometer "slide" via a wire with a small electronic clip, 0.5 mm wide, and this clip was moved along the wire to vary the resistance. The nominal resistance of the wire was 61 mΩ/m. The resistance of an identical, 3 m long, wire was measured with the 4-wire technique using an Agilent 34401A DMM. It was measured to 63 mΩ/m (indicating a true diameter of 0.598 mm). This measured value 63 mΩ/m was used to calibrate the digital ohmmeter. (Compare this number to expression (14); theoretically this predicts that changes in the wire length of the order of 1 mm can be detected! This was indeed confirmed experimentally.)

A C-compiler from HI-TECH, PICC-18,[24] was used to write a C-program according to the flowchart in Figure 5. (A C-routine was added that transfers data (s_{total}/500) via an asynchronous serial link to the host PC at a baud rate of 19 200 bits/s).

V. EXPERIMENTAL RESULTS

R_X was varied by moving the small electronic clip along the copper wire (= the "potentiometer slide"). The length of the wire was measured with a caliper with vernier scale and the length was converted into resistance by using the measured conversion factor 63 mΩ/m. For each R_X value, the host PC registered the ADC integer and the result is illustrated in Figure 9.

Notice that the gradient, 17.98 counts/mΩ, corresponds to a resistance resolution of 55.6 $\mu\Omega$/count, which is even better than the theoretically predicted 74.5 $\mu\Omega$/count. (This will be commented on that later.) Figure 10 is an enlarged view of the low-resistance end of Figure 9 where the sensitivity is seen to decrease at the low end; below 3 mΩ the gradient is only 14.7 counts/mΩ corresponding to a resolution of 68 $\mu\Omega$/count.

In order to determine the sample-to-sample fluctuations, the firmware was changed so that each sample was

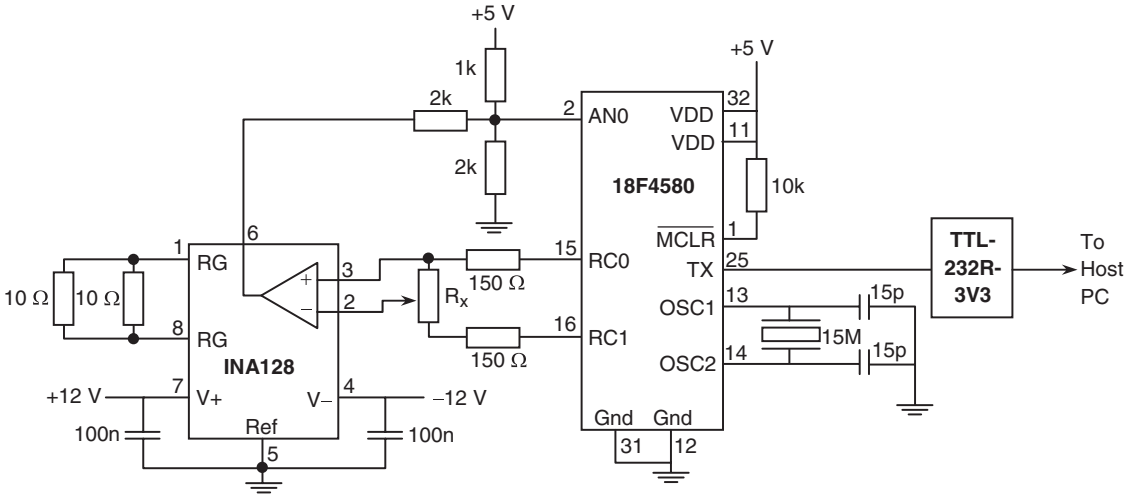

FIG. 8. The digital milli-ohmmeter hardware.

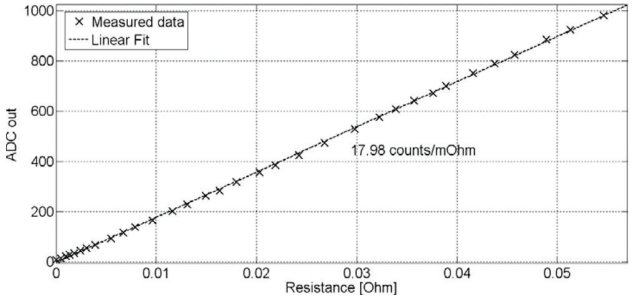

FIG. 9. Digital milli-ohmmeter with digital lock-in technique.

transferred to the host PC (Figures 9 and 10 present the averaged values only). This revealed that the (relative) variance of the sample-to-sample fluctuations was largest for the low-Ω range but stabilized to an almost constant value for larger Ω-values. Table II illustrates the relative sample-to-sample fluctuations for a few resistance values (i.e., the standard deviation divided by the sample value, σ/x).

Since the "real" application produces the average of 500 samples, the standard deviation of s_{total} is $\sigma/\sqrt{500}$ as expected for a normal distribution. These values are presented in column 3 in Table II for a few resistance values. Figure 11 illustrates the relative uncertainty due to stochastic fluctuations in the same diagram as the resistance measurement (multiplied by a factor of 10^5).

The lock-in frequency is determined by the time consumed by the inner loop in Figure 5 and was measured to 141.25 Hz. This could easily be adjusted but the observed SNR did not indicate a need to change the lock-in frequency.

VI. DISCUSSION

The experimental data deviated some from the predictions. The experimental resolution of 55.6 $\mu\Omega$/count is 30% better than the theoretically expected 74.5 $\mu\Omega$/count. Also, as illustrated in Figure 10, the sensitivity decreases for very low resistances. Below 3 mΩ, the resolution is 68 $\mu\Omega$/count, which is very close to the theoretical value.

The reasons for the deviations lie mostly in the non-ideal response of the instrumentation amplifier. The magnitude of the voltage drop across the resistor R_X should be independent of the current direction. (There was no detectable difference in the output current from the two I/O-pins or in the output impedances.) Ideally, the instrumentation amplifier's

TABLE II. Relative fluctuations.

Resistance (mΩ)	Relative σ (%) Sample-to-sample	Relative σ (%) 500 averages
0.504	9.57	0.43
9.954	1.50	0.067
33.39	1.47	0.066
50.65	1.73	0.077

gain should be the same for both $+U_X$ and $-U_X$ over the entire input range. This particular application depends on the sum of A^+_{NM} and A^-_{NM} (see expression (10)) and these amplifications, and the sum of them, were investigated experimentally. Data showed that for "large" signal inputs ($R_X > 3$ mΩ), the sum of A^+_{NM} and A^-_{NM} was 25%–30% larger than nominal, i.e., ∼25 000 times instead of the nominal 20 000 (and $A^+_{NM} \approx A^-_{NM}$). However, for "small" signal inputs ($R_X < 3$ mΩ), both A^+_{NM} and A^-_{NM} decreased (A^+_{NM} decreased more than A^-_{NM}) and the sum of them approached the nominal 20 000).

This deviation of the amplification from the nominal value also explains why the theoretical resistance value for $s = 512$ (in Table I), does not agree with the diagram in Figure 9; the uncertainty budget uses nominal values for the amplification.

Some attempts were made to compensate for the deviation of A^+_{NM} from A^-_{NM} by making the bipolar supply voltage slightly unsymmetrical but that was unsuccessful. Also, 100 kΩ resistors to ground were added on each input to make sure that there was a safe return path for the input bias current. This had no effect either (which was really not expected;[25] the input bias current can return to ground via either one of the R_0/R_1 resistors). The conclusion is that for accurate measurements, the system has to be carefully calibrated for each individual amplifier. The error analysis (and data) also illustrates that it is the uncertainty in the amplification factors that limit the accuracy of the absolute resistance measurement.

It can be seen from Figure 11 that the relative uncertainty due to stochastic fluctuation is almost constant for resistance values above 5 mΩ suggesting a constant signal-to-noise ratio (SNR). This SNR depends on the number of samples averaged. Table II indicates that the sample-to-sample SNR is ∼1/0.015 ≈ 65 but decreases rapidly for very small resistances. However, the fluctuations are stochastic and have

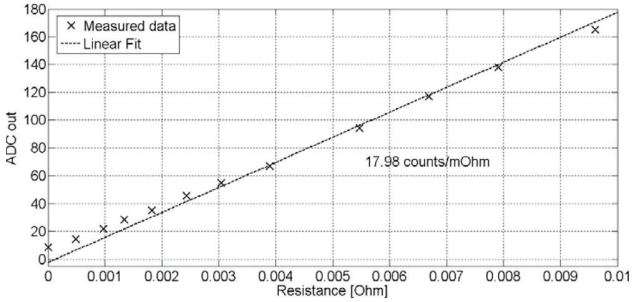

FIG. 10. The detector is less sensitive at the low end.

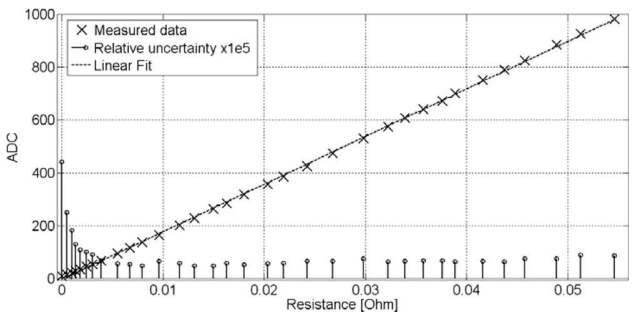

FIG. 11. The relative uncertainty for each sample.

a Gaussian distribution; the SNR can be improved arbitrarily (down to the ADCs quantization limit) by averaging. The "cost" for improving the SNR by averaging is of course a decrease in the throughput performance (decreased bandwidth).

The lock-in frequency range depends on the instrumentation amplifier's settling time after each switching of the I/O-pins output and enough time must be allowed for settling before the AD conversion is initiated. The settling time was experimentally determined; at least 450 μs should be allowed for settling before AD conversion starts. Hence, the maximum lock-in frequency is

$$f_{\text{lock-in}}^{\max} = \frac{1}{2 \times (450 + 48) \times 10^{-6}} \approx 1\text{kHz}. \quad (15)$$

(An AD conversion takes 48 μs.) This frequency corresponds to half the bandwidth of the amplifier when the differential gain is 10 000.

VII. CONCLUSIONS

There are plenty of situations that depend on accurate sub-milliohm measurements.[1,4,26–29] This includes measuring the resistance of switch and circuit breaker contacts, transformer and motor windings, weld and soldering bonds in aircrafts, rail and pipes, cable splices, fuses, metal alloys, cables, etc. Accurate resistance measurements are also necessary for measuring cryogenic temperatures,[4] heat capacity in calorimeters,[27] corrosion of boat carcass and car chassis,[28] and for monitoring degradation in pressure-junctions.[29] The price of a commercial, hand-held field-ohmmeter with micro-ohm resolution is somewhere in the range of $500–$1000.[30] For a desktop instrument, you might have to pay three or four times of that.

This work has demonstrated how an ohmmeter with a resolution of less than 60 $\mu\Omega$ can be designed with a general purpose microcontroller and an instrumentation amplifier at a component cost of the order of $30. The design is presented in detail in Figure 8. When measuring very low resistances, care must be taken to avoid the influence of cable resistances, contact resistances due to surfaces roughness[31] or oxide layers[32] and Seebeck thermocouple effects. All these potential interferences are eliminated in this design by a combination of techniques; a Kelvin probe is used to cancel cable and contact resistances, the fact that the current is reversed through the sample and that two samples of opposite sign are subtracted cancels thermo emfs and the phase lock-in design makes it possible to selectively detect the microvolt drop across the sample in spite of the presence of inherent noise sources such as Johnson noise and 1/f noise.

The reported <60 $\mu\Omega$ resolution should be compared with the (typical) measurement uncertainty of 0.32 mΩ for absolute measurements (see Table I). As the uncertainty analysis showed, it is the uncertainty in the differential gain of the instrumentation amplifier that is the main uncertainty contribution; for accurate absolute measurements, a careful calibration is required and a look-up table should be implemented in firmware to instantly produce absolute resistance values. For accurate absolute measurements, it will also be necessary to monitor the ambient temperature and offset voltage trimming circuitry should be added; when the input terminals are short-circuited the output signal should be adjusted to 0 V. According to the data sheet,[22] most applications do not require that, but for very-low absolute resistance measurements this should be considered; however, it adds an OP amp, two current sources, and a few resistors to the design.[22]

Since this application measures real (non-complex) impedance, there was no need for phase compensation. In another application, where the detection electronic introduces a phase shift between the reference signal and the measurement signal, phase compensation may be necessary. This could easily be added to the design. Either by adding a potentiometer to a second analog input whose reading could be used to vary the phase shift, or the algorithm suggested by Li *et al.*[18] could be used to find the in-phase and quadrature components by increasing the sampling rate in order to have a sampling time corresponding to $\pi/2$ (relative the reference signal).

The proposed solution is a considerable improvement and compared other similar suggested implementations of digital LIAs (Refs. 2 and 19) since it does not need an external waveform generator to excite the experiment and is considerably less expensive than commercial LIAs or LIAs implemented in software on Windows computers.

[1] J. L. Scott, "Introduction to lock-in amplifiers," DL Instruments Technical Notes IAN47, 2002, see http://www.dlinstruments.com/technotes/index.html.

[2] A. Restelli, R. Abbiati, and A. Geraci, Rev. Sci. Instrum. **76**, 09312 (2005).

[3] M. J. Schauber, S. A. Newman, L. R. Goodman, I. S. Suzuki, and M. Suzuki, Am. J. Phys. **76**(2), 129–132 (2008).

[4] X. G. Feng, S. Zelakiewicz, and T. J. Gramila, Rev. Sci. Instrum. **70**(5), 2365–2371 (1999).

[5] S. Wolf and R. F. M. Smith, *Electronic Instrumentation Laboratories*, 2nd ed. (Prentice-Hall, Upper Saddle River, New Jersey, 2004).

[6] K. D. Wong, *Accurate Milliohm Measurement*, 2011, see http://www.kerrywong.com/2011/08/14/accurate-milliohm-measurement/.

[7] Stanford. *About Lock-In Amplifiers*, Stanford Research Systems, Application Note #3, 2006, see http://www.thinksrs.com/downloads/PDFs/ApplicationNotes/AboutLIAs.pdf.

[8] J. Stoltenberg and O. E. Vilches, *Introduction to the Phase Sensitive (Lock-In) Detector*, 1997, see http://advancedlab.org/mediawiki/index.php/Appendix_D:the_Phase_Sensitive_%28Lock-In%29_Detector.

[9] E. H. Fisher, *The Evolution of the modern Lock-in Amplifier*, DL Instruments Technical Notes IAN35, 2003, see http://www.dlinstruments.com/technotes/index.html.

[10] D. Abramowitch, "Phase-locked loops: A control centric tutorial," in *Proceedings of the 2002 ACC*, Anchorage, Alaska, USA, 2002, see http://dabramovitch.com/pubs/pll_tutorial.pdf.

[11] R. Wolfsson, Am. J. Phys. **59**, 569–572 (1991).

[12] T. Tashev, "Signal measuring instrument lock-in amplifier," in *Proceedings of the 7th WSEAS Conference Circuits, Systems, Electronics, Control and Signal Processing, (CSECS'08)* (WSEAS Journals, Puerto De La Cruz, Canary Islands, Spain, 2008), pp. 243–245.

[13] J. Quin, Z. Huang, Y. Ge, Y. Hou, and J. Chu, Rev. Sci. Instrum. **80**, 033112 (2009).

[14] D. Wu, C. Wang, H. Sun, and H. Wang, "A novel digital lock-in amplifier with dual channels," in *Proceedings of the 2009 International Asia Conference on Informatics in Control, Automation and Robotics*, Bangkok, Thailand, 2009.

[15] F. Momo, G. A. Ranieri, A. Sotgui, and M. Terenzi, J. Phys. E: J. Sci. Instrum. **14**, 1253–1256 (1981).

[16] X. Wang, Rev. Sci. Instrum. **61**(7), 1999–2001 (1990).

[17] W. Yiding, W. Yunhong, and Z. Shi, "Errors analysis of spectrum inversion methods," in *Proceedings of the 2007 IEEE International Conference on Signal Processing and Communications (ICSPC 2007), Dubai, United Arab Emirates, November 24-27, 2007*, see http://ieeexplore.ieee.org/stamp/stamp.jsp?tp=&arnumber=4728304.

[18]G. Li, M. Zhou, F. He, and L. Lin, Rev. Sci. Instrum. **82**, 095106 (2011).
[19]Z. Gao, H. Zheng, L. Li, F. Chen, and F. Guo, "A single channel input virtual dual-phase lock-in amplifier," in *Proceedings of the 2011 International Conference on Optical Instruments and Technology* (SPIE, Beijing, China, 2011), Vol. 8197, p. 81971F.
[20]Microchip, "PIC18F2480/2580/4480/4580 Data Sheet," Microchip, Inc., DS39637D, Tuscon, Arizona, 2009, see http://ww1.microchip.com/downloads/en/DeviceDoc/39637d.pdf.
[21]D. Greggio, "Microchip forums," Microchip, Inc., 2011, see http://www.microchip.com/forums/m621050-print.aspx.
[22]Burr-Brown, *INA128/INA129: Precision, Low Power Instrumentation Amplifiers*, 1995, see http://www.ti.com/lit/ds/symlink/ina128.pdf.
[23]FTDI, "TTL to USB serial converter range of cables," Future Technology Devices International Ltd, 2010, see http://www.ftdichip.com/Support/Documents/DataSheets/Cables/DS_TTL-232R_CABLES.pdf.
[24]HI-TECH, *HI-TECH C tools for the PIC18 MCU Family*, 2011, see http://ww1.microchip.com/downloads/en/DeviceDoc/PICC_18_9_80_manual.pdf
[25]C. Kitchin and L. Counts, *A Designer's Guide to Instrumentation Amplifiers*, 3rd ed., Analog Devices, 2006, see http://www.analog.com/static/imported-files/design_handbooks/5812756674312778737Complete_In_Amp.pdf.
[26]Albercorp, *Micro-ohmmeters, Low Resistance Testers*, 2004, see http://www.alber.com.cn/BrochuresPDF/MOMpb.pdf.
[27]Z.-C. Tan, Q. Shi, B.-P. Liu, and H.-T. Zhang, J. Therm. Anal. Calorim. **92**(2), 367–374 (2008).
[28]A. R. Wilson, and R. F. Muscat, Sens. Actuators, A **169**, 301–307 (2011).
[29]D. G. Loucks, IEEE Trans. Ind. Appl. **47**(2), 688–694 (2011).
[30]Cropico, *DO4000 Series*, 2011, see http://www.farnell.com/datasheets/391379.pdf.
[31]R. S. Timsit, *Electrical Contact Resistance: Review of Elementary Concepts*, 2012, see http://www.connectorsupplier.com/tech_updates_Timron_ElectricalContactResistance_1-23-07.htm.
[32]J. Kister, "Introduction to the physics of contact resistance," Probe Technology, SouthWest Test Workshop, San Diego, 1998, see http://www.swtest.org/swtw_library/1998proc/PDF/S01_kister.PDF.
[33]T. M. Adams, *G104-A2LA Guide for Estimation of Measurement Uncertainty in Testing*, 2002, see http://www.a2la.org/guidance/est_mu_testing.pdf.
[34]S. Bell, *A Beginner's Guide to Uncertainty of Measurement*, 2009, see http://www.wmo.int/pages/prog/gcos/documents/gruanmanuals/UK_NPL/mgpg11.pdf.
[35]F. Reverter, J. Jordana, M. Gasulla, and R. Pallàs-Areny, Sens. Actuators, A **121**, 78–87 (2005).